

# Generic Contrast Agents

Our portfolio is growing to serve you better. Now you have a *choice*.



[VIEW CATALOG](#)

# AJNR

This information is current as of May 22, 2025.

## **Physiologic and Anatomic Assessment of a Canine Carotid Artery Stenosis Model Utilizing Phase Contrast with Vastly Undersampled Isotropic Projection Imaging**

A.S. Turk, K.M. Johnson, D. Lum, D. Niemann, B. Aagaard-Kienitz, D. Consigny, J. Grinde, P. Turski, V. Haughton and C. Mistretta

*AJNR Am J Neuroradiol* 2007, 28 (1) 111-115

<http://www.ajnr.org/content/28/1/111>

ORIGINAL  
RESEARCH

A.S. Turk  
K.M. Johnson  
D. Lum  
D. Niemann  
B. Aagaard-Kienitz  
D. Consigny  
J. Grinde  
P. Turski  
V. Haughton  
C. Mistretta

# Physiologic and Anatomic Assessment of a Canine Carotid Artery Stenosis Model Utilizing Phase Contrast with Vastly Undersampled Isotropic Projection Imaging

**BACKGROUND AND PURPOSE:** Noninvasive assessment of the hemodynamic significance of carotid stenosis is often performed with MR angiography and supplemented with carotid Doppler sonography. Phase contrast with vastly undersampled isotropic projection reconstruction (PC-VIPR), a novel MR imaging technique, accelerates phase-contrast MR flow imaging and provides both images of the vessels and measurements of blood-flow velocities. For this study, we determined the accuracy of PC-VIPR blood-flow velocity measurements to determine pressure gradients across an experimental carotid stenosis.

**MATERIALS AND METHODS:** A focal stenosis was surgically created in each common carotid artery of 6 canines. Digital subtraction angiography (DSA) was performed, and the degree of stenosis was determined using the North American Symptomatic Carotid Endarterectomy Trial methodology. A microcatheter was positioned in the carotid artery proximal and distal to the stenosis, and pressures were measured in the vessel through the catheter. PC-VIPR was then performed on a 1.5T MR imaging scanner with parameters producing 0.8-mm isotropic voxel resolution. From the velocity measurements, pressure gradients were calculated from the Navier-Stokes relationship to compare with the pressures measured by a catheter.

**RESULTS:** Carotid stenoses in the 50%–85% range were produced in the 12 arteries. Pressure gradients across the stenoses ranged from 6 to 26 mm Hg. The pressure gradient calculated from the PC-VIPR data correlated ( $r = 0.91$ ,  $P < .0001$ ) with the actual pressure measurements.

**CONCLUSION:** With PC-VIPR, a novel MR imaging technique, the hemodynamic effect of a stenosis on flow and pressure can be evaluated.

Stroke is the third leading cause of death and disability in the United States, with more than 700 000 new strokes occurring each year.<sup>1</sup> Up to 25% of these strokes are related to stenosis of the carotid arteries.<sup>1</sup> Because of the significant impact on patient outcomes, much work has been done over the past 20 years to reduce this effect. Many clinical trials such as the North American Symptomatic Carotid Endarterectomy Trial (NASCET),<sup>2</sup> the European Carotid Surgery Trial (ECST),<sup>3</sup> and the Veteran Affairs Cooperative Trial<sup>4</sup> have demonstrated that surgical revascularization of the stenosis will reduce the future stroke risk in certain patient populations, related to degree of narrowing. Because of the correlation of patient risk reduction in groups harboring a certain degree of stenosis, it is paramount to be able to accurately and noninvasively determine the degree of stenosis.

Clinical evaluation of carotid stenosis has changed very little during the last decade with correlation of 2 noninvasive studies such as MR angiography (MRA) and carotid Doppler sonography being the recommended preoperative imaging techniques.<sup>5–7</sup> In the interventional coronary literature, previous work has been performed that demonstrated that measurable pressure gradients can be useful to determine the significance of a stenosis.<sup>8–10</sup> Evaluation of iliac and renal stenosis

has similarly shown that pressure gradients can help further determine the significance of a stenosis.<sup>11–16</sup> However, these measurements were performed during angiography, requiring an invasive procedure, and are not practical in the carotid arteries, in which there is an increased risk of a thromboembolic event when the stenosis is crossed with a wire or microcatheter.

We have developed a novel method for obtaining phase-contrast images with phase-contrast with vastly undersampled isotropic projection reconstruction (PC-VIPR).<sup>17,18</sup> Using this method, we can obtain anatomic images with similar resolution to standard 3D time-of-flight (TOF) examinations, but with greater anatomic coverage. Additionally, 3-directional velocity images are obtained at up to 50 times faster than conventional 3D Cartesian phase-contrast examinations when one is considering acquisition time, voxel size, and anatomic coverage. This rapid imaging technique can also be used in conjunction with cardiac gating to generate quantitative time-resolved blood-flow measurements in clinically feasible imaging times. This time-resolved information can be retrospectively analyzed to calculate intravascular pressure gradients.

Given the current clinical absence of a noninvasive gold standard method of imaging, we believe that MR imaging may achieve this status if supportive physiologic data can improve the anatomic accuracy of determining the significance of a stenosis. For this study, we wanted to determine the feasibility of the PC-VIPR sequence to measure pressure gradients across an experimental canine carotid stenosis.

Received December 6, 2005; accepted after revision February 27, 2006.

From the Departments of Radiology (A.S.T., D.L., D.N., B.A.-K., D.C., J.G., P.T., V.H.), Medical Physics (K.M.J., C.M.), and Neurosurgery (A.S.T., D.N., B.A.-K.), University of Wisconsin Hospital and Clinics, Madison, Wis.

Please address correspondence to: Aquilla S. Turk, DO, 600 Highland Ave, CSC E3/372, Madison, WI 53792; e-mail: as.turk@hosp.wisc.edu

## Materials and Methods

### Surgery and Angiography

The protocol for the study was approved by the institutional animal care committee. Six female beagles weighing approximately 30 pounds each underwent surgery to create common carotid artery stenoses. All surgeries were performed with the animals under general endotracheal anesthesia. A plastic nonferromagnetic cable tie was secured around each carotid artery. One week of recovery was allowed to resolve any evidence of vasospasm or irritative effects of the surgery. The common carotid arteries all measured between 3.5 and 4 mm in diameter.

With the animals under general anesthesia and by using standard techniques, a digital subtraction angiogram (DSA) was obtained in the frontal and lateral projections of the carotid arteries. Digital images documented the degree of stenosis by using methods outlined in the NASCET trial.<sup>2</sup> An Excel-14 microcatheter (lumen diameter, 0.017 inches; Boston Scientific Corp, Fremont, Calif) was then manipulated under fluoroscopic monitoring into a position 1 cm proximal to the stenosis and connected to a Propaq arterial pressure monitor (Protocol Systems, Beaverton, Ore). Systolic, diastolic, and mean arterial pressures were observed for a period of 2 minutes to observe stability of the reading. Arterial waveforms were observed to ensure consistency and appropriate catheter readings. The data were then recorded with the corresponding arterial waveform, the catheter was manipulated into a position at the stenosis and subsequently 1 cm distal to the stenosis, and the sequence repeated. The pressure gradient across the stenosis was calculated by subtracting the mean pressure distal to the stenosis from the mean pressure proximal to the stenosis.

### MR Imaging

With the animal still under anesthesia and the catheter removed, the beagle was placed in a 4-channel knee coil and imaged with a 1.5T MR imaging scanner (TwinSpeed Excite HD, Version 12.0, GE Healthcare, Waukesha, Wis). Electrocardiogram (ECG) leads were placed. Standard contrast-enhanced and 3D TOF images were obtained. PC-VIPR was acquired with ECG gating at the following parameters: TE/TR of 3.4/8.8 ms and temporal resolution of 40 ms,  $256 \times 256 \times 256$  acquisition matrix,  $20 \times 20$  cm FOV, 15-cm z-axis excitation slab, 32-kHz readout bandwidth, 75% fractional readout, and a velocity-encoding value of 150 cm/s. The total imaging time for the PC-VIPR scan was 10 minutes, 14 seconds. Voxel sizes of the TOF and contrast-enhanced examinations were  $0.7 \times 0.7 \times 1.4$  mm and  $0.5 \times 0.5 \times 2.0$  mm, respectively, compared with  $0.78125 \times 0.78125 \times 0.78125$  mm ( $0.477 \text{ mm}^3$ ) in the PC-VIPR examination. Data at individual timeframes within the cardiac cycle were reconstructed by using an adaptive-width temporal filter. Each image was reconstructed by using the central portions of *k*-space sampled during a narrow time segment and the periphery of *k*-space sampled from a broader temporal window. For each timeframe, dynamic velocity images were reconstructed via phase-difference processing. Anatomic images were processed from the composite complex difference volumetric dataset.

Dynamic phase-difference images were then analyzed to determine flow rates and trans-stenotic pressure gradients. Flow rates across the stenosis were measured by using a standard GE flow analysis package on the axial flow images. Pressure gradients were determined on the basis of iterative methods that have been validated in both phantom and animal models.<sup>19-22</sup> This technique is based on the Navier-Stokes equations, which simplify more complex relationships

by assuming the fluid to be both incompressible and Newtonian. Arterial blood flow generally satisfies these assumptions with a dynamic viscosity of approximately 4 cP. A 4-step process was used in the implementation of the technique, consisting of vessel segmentation, pressure-gradient determination, integrative pressure determination, and iterative refinement. Vessel segmentation was performed with a user set threshold, which was followed by an anti-island filter. This filter smoothed the vessel wall and removed small isolated regions that cloud images and introduce additional error. Pressure gradients were then determined by using central difference equations with corrections for errors occurring at the edge of the vessel. Next, an initial pressure map was determined by using a simple seed-point method and was iteratively refined by using a path-averaging algorithm.<sup>19</sup> Dynamic pressure maps were then averaged for comparison with *in vivo* measurements, and the calculation of pressure from the PC-VIPR data was compared with the pressure differences that were measured between 1 cm proximal and 1 cm distal to the stenosis.

### Data Evaluation

The degree of carotid stenosis was estimated on the basis of the NASCET criteria from the projection with the most significant stenosis.<sup>2</sup> The measurements were performed by printing the image and measuring the vessel with calipers. Pressure gradients calculated from the PC-VIPR data were compared with the actual pressure measurement (catheter) with regression analysis.

### Statistics

The calculated pressure gradients were compared with the actual pressure gradients (catheter measurement), and the correlation was tested with a Z-test by using Fisher *r* to *z* transformation. Further agreement between the pressure measurements was evaluated by using 95% confidence intervals (CIs) on the difference of the values as described by Bland and Altman.<sup>23,24</sup>

### Results

In the 6 canines, DSA, catheter pressure measurements, contrast-enhanced MR images, TOF MR images, and PC-VIPR images were acquired and were deemed technically adequate. The animals demonstrated no evidence of complication from angiography.

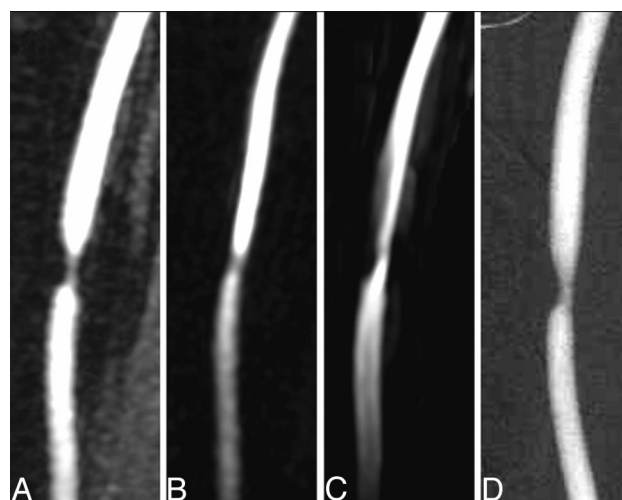


**Fig 1.** Sample carotid stenosis images from contrast-enhanced MRA (A), PC-VIPR MRA (B), 3D Time of Flight MRA (C), and DSA (D).

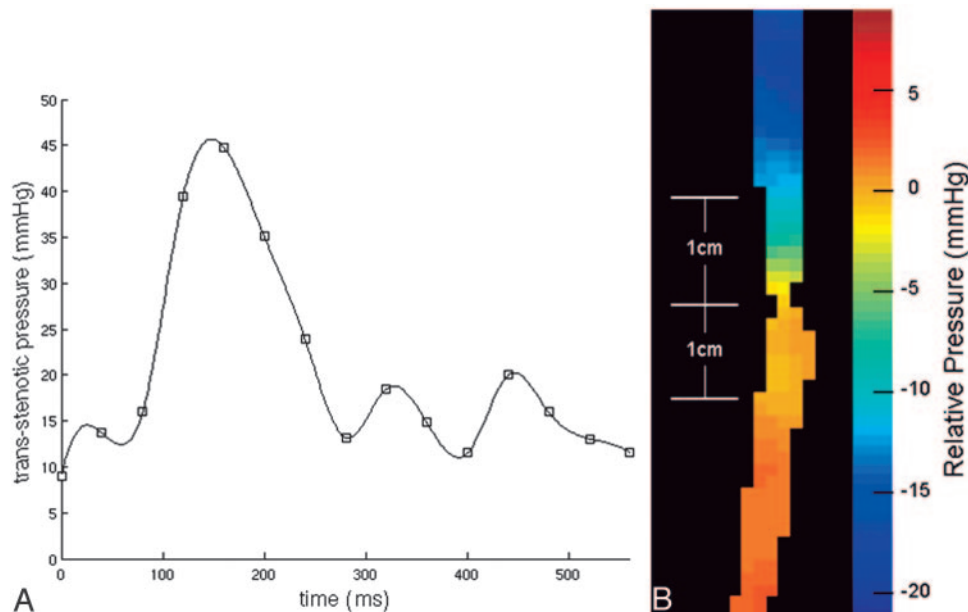


**Fig 2.** Sample dynamic pressure curve (A) and average pressure color map (B) from the PC-VIPR technique obtained across the carotid artery stenosis.

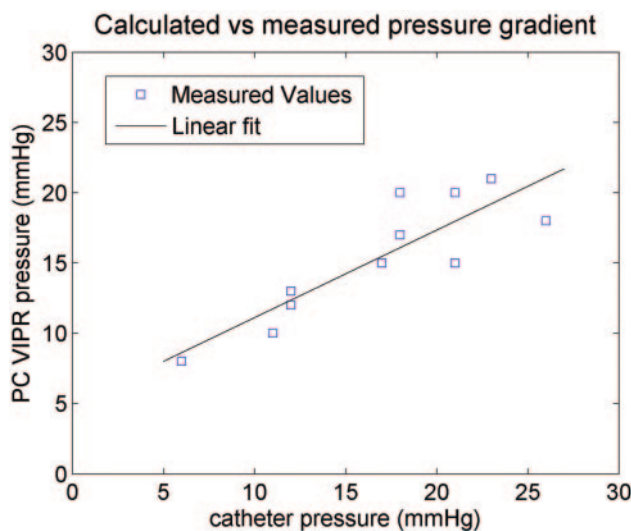


**Fig 3.** Plot showing correlation of actual measured microcatheter values versus calculated pressure gradients from PC-VIPR across the stenosis.

DSA showed a smoothly tapering carotid stenosis in each carotid artery, ranging from 50%–85%. In 1 carotid artery with 85% stenosis, signal-intensity loss present at the stenosis on MR imaging precluded an accurate evaluation of the stenosis with PC-VIPR. In the other cases, the stenosis demonstrated in the DSA was also demonstrated with the conventional MRA techniques and with PC-VIPR (Fig 1).

In each carotid artery, pressure waveforms similar to those from direct invasive monitoring were obtained with the time-resolved PC-VIPR data (Fig 2A). Pressure maps created from the velocity data showed pressure drops across the carotid stenosis (Fig 2B). The pressure gradient over the stenosis calculated from the PC-VIPR data for the 12 carotid arteries ranged from 8 to 20 mm Hg.

The Z-test showed a high degree of correlation ( $r = 0.86$ ,  $P = .0006$ ) in the pressure gradients obtained noninvasively with PC-VIPR and invasively with a microcatheter (Fig 3).

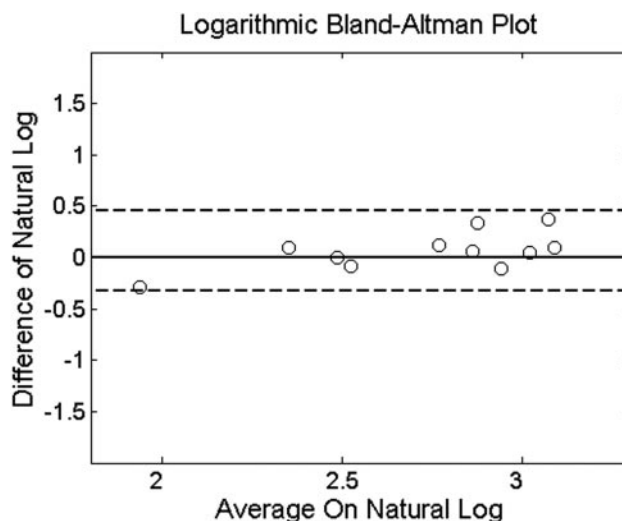


**Fig 4.** Bland-Altman plot showing the correlation of the logarithm-transformed actual measured microcatheter values versus the logarithm-transformed calculated pressure gradients from PC-VIPR across the stenosis. Dashed line represents the 95% CI at  $-0.33$  and  $0.46$ .

Figure 3 also shows inflation of variance as the pressure values increase; thus, we used the logarithm-transformed data to smooth the variance.<sup>23,24</sup> We obtained a 95% CI for the logarithm of the pressure gradients measured from the catheters subtracted from the logarithm of the calculated PC-VIPR measurements ( $-0.33$ ,  $0.46$ ). This means that 95% of the VIPR measurements are expected to be 0.72–1.58 times the corresponding catheter measurements. The correlation between the logarithm-transformed pressure measurements was  $0.91$  ( $P < .0001$ ) (Fig 4).

Microcatheter pressure tracings showed systolic and diastolic variations with minimal deviation during the period of recording pressure in each animal. These variations due to systole and diastole were greater proximal to the stenosis than distal to it (Fig 5). Differences in mean arterial pressure prox-



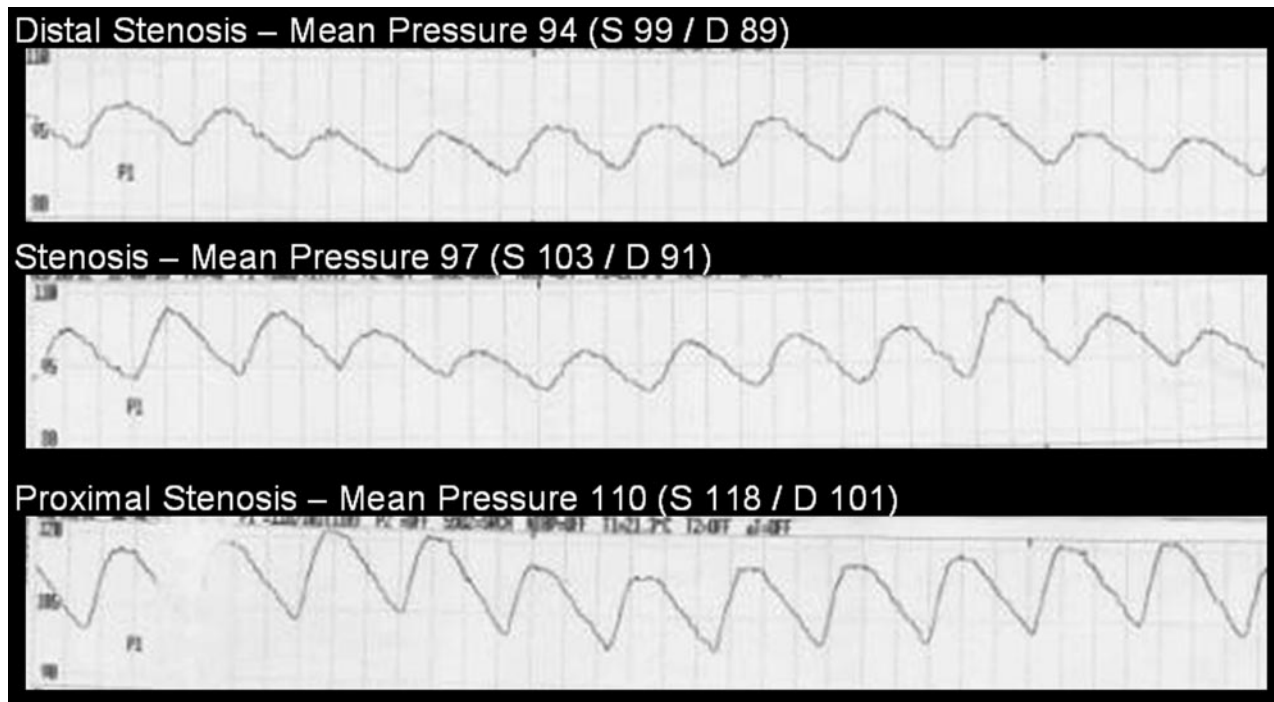


**Fig 5.** Sample arterial waveform tracings from the microcatheter at least 1 cm distal to the carotid stenosis (top row), at the level of the stenosis (middle row), and at least 1 cm proximal to the stenosis (bottom row). The adjacent values represent the mean arterial pressures as well as the systolic (S) and diastolic (D) values generated by the Propaq arterial pressure monitor.

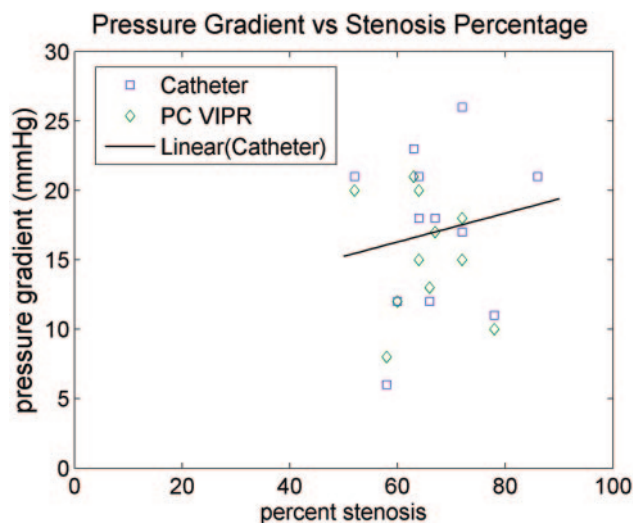


**Fig 6.** Plot showing that pressure changes are identified at all of the observed degrees of stenosis with weak correlation between the degree of stenosis and the pressure gradient due to a high variability in pressure changes.

imal and distal to the stenosis ranged from 6 to 26 mm Hg in the 12 carotid arteries. The pressure gradient and the degree of stenosis did not correlate closely (Fig 6).

## Discussion

This study shows that in animals with surgically induced carotid stenosis greater than 50%, PC-VIPR can demonstrate the stenosis and estimate the physiologic significance of the stenosis. This study in animals was performed as a proof of the principle that a fast phase-contrast MR imaging technique with good temporal and spatial resolution demonstrates both the anatomic changes in the vessel and their effect on flow. The

number of animals was limited but highly significant correlations ( $r = 0.91$ ,  $P < .0001$ ) were found between the pressure gradients calculated from the PC-VIPR sequence and the pressures gradients measured with a catheter.

PC-VIPR is novel phase-contrast MR imaging technique designed to purposefully undersample the periphery of  $k$ -space, which allows image-acquisition rates up to 50 times faster than standard Cartesian imaging.<sup>17,18</sup> By design, this technique yields increased spatial resolution and greater anatomic coverage. Quantitative flow and velocity information is the underlying strength of phase-contrast techniques. This allows mathematic analysis of the data with the Navier-Stokes equation to generate pressure gradients across the region of stenosis.

One of the weaknesses of this study is that the stenosis produced surgically in these animals does not replicate the stenoses resulting from atherosclerosis. The longer irregular stenosis in patients with atherosclerosis may result in different flow patterns than those in this study. Although the pressure gradients calculated from PC-VIPR correlated well with the pressure gradients measured, those calculated from PC-VIPR had a smaller range. Although in the PC-VIPR measurements the range was 8–20 mm Hg, in the actual recordings it was 6–26 mm Hg. Which measurement of pressure in this study was more accurate cannot be determined. Possible explanations include damping of the pressure measurement in the catheter system or partial volume averaging effects in the PC-VIPR flow data.

Furthermore, the effect of the long TE on the accuracy of flow measurements in the face of very complex flow is not known. PC-VIPR is relatively insensitive to dephasing from turbulent flow because of the high resolution and isotropic acquisition of the PC-VIPR pattern. We have tried to reduce

the TE by using balanced gradients and a fractional readout, which may result in a small increase in error or possible failures in complex flow. However, we have found that the size of the vessel is more important than tortuosity or the complexity flow for success with this sequence.

Results from this study agree well with those of other studies in which pressure gradients have been made. In this study, pressure gradients of up to 26 mm Hg were present in the stenoses that were surgically induced. In renal arteries, a pressure gradient of more than 20 mm Hg was shown to have clinical significance.<sup>11</sup> In the iliac arteries, stenoses have been reported to be significant at 5–10 mm Hg.<sup>12,13</sup>

It has been well documented that stenosis of  $\geq 70\%$  can cause signal-intensity dropout at the site of stenosis on standard 3D TOF MRA.<sup>25,26</sup> This occurred once in this study as well as in some of our preliminary work. When it occurred, there was failure of the PC-VIPR to produce a flow or pressure-gradient result because of a loss of data at the stenosis site. During our development of the PC-VIPR sequence, we improved the resolution by decreasing the FOV, resulting in smaller isotropic voxels (0.78125 mm), which have helped to minimize this artifact. However, clinically this change very likely will not result in a significant problem because it has been well established that symptomatic patients with stenosis  $\geq 70\%$  should undergo surgery.<sup>2,3</sup> The stenoses that result in a 50%–70% narrowing are the group that requires further characterization.

PC-VIPR allows MR imaging to provide further physiologic data about a stenosis. Given the varied pressure gradients at which stenoses are deemed significant, depending on anatomic location, we are uncertain of the level of pressure change at which a carotid stenosis will become significant. In the future, we hope to establish with further studies that a threshold exists at which the pressure gradient, as determined by PC-VIPR, becomes significant, such as is seen with duplex sonographic velocities.

## Conclusion

PC-VIPR, a novel MR imaging technique, can yield trans-stenotic gradient pressures that highly correlate with those obtained invasively. This result allows the degree of stenosis of a vessel and the effect of the stenosis on flow to be evaluated with a single technique. Coupling physiologic and anatomic data may improve accuracy and consolidate noninvasive imaging evaluation of arterial stenosis. Further work in this area is currently underway.

## References

1. American Heart Association. *Heart Disease and Stroke Statistics—2005 Update*. Dallas: American Heart Association; 2005
2. Barnett HJ, Taylor DW, Eliasziw M, et al. Benefit of carotid endarterectomy in

- patients with symptomatic moderate or severe stenosis: North American Symptomatic Carotid Endarterectomy Trial Collaborators. *N Engl J Med* 1998;339:1415–25
3. Randomised trial of endarterectomy for recently symptomatic carotid stenosis: final results of the MRC European Carotid Surgery Trial (ECST). *Lancet* 1998;351:1379–87
4. Mayberg MR, Wilson SE, Yatsu F, et al. Carotid endarterectomy and prevention of cerebral ischemia in symptomatic carotid stenosis: Veterans Affairs Cooperative Studies Program 309 Trialist Group. *JAMA* 1991;266:3289–94
5. Turnipseed WD, Kennell TW, Turski PA, et al. Magnetic resonance angiography and duplex imaging: noninvasive tests for selecting symptomatic carotid endarterectomy candidates. *Surgery* 1993;114:643–48
6. Patel MR, Kuntz KM, Klufas RA, et al. Preoperative assessment of the carotid bifurcation: Can magnetic resonance angiography and duplex ultrasonography replace contrast arteriography? *Stroke* 1995;26:1753–58
7. Nederkoorn PJ, Mali WP, Eikelboom BC, et al. Preoperative diagnosis of carotid artery stenosis: accuracy of noninvasive testing. *Stroke* 2002;33:2003–08
8. Pijls NHJ, Gelder BV, Pepijn VV, et al. Fractional flow reserve: a useful index to evaluate the influence of an epicardial coronary stenosis on myocardial blood flow. *Circulation* 1995;92:3183–93
9. Prendergast BD, Kerr F, Starkey IR. Normalization of abnormal coronary fractional flow reserve associated with myocardial bridging using an intracoronary stent. *Heart* 2000;83:705–07
10. Aude YW, Garza L. How to prevent unnecessary coronary interventions: identifying lesions responsible for ischemia in the cath lab. *Curr Opin Cardiol* 2003;18:394–99
11. Gross CM, Kramer J, Weingartner O, et al. Determination of renal arterial stenosis severity: comparison of pressure gradient and vessel diameter. *Radiology* 2001;220:751–56
12. Murphy KD, Encarnacion CE, Le VA, et al. Iliac artery stent placement with the Palmaz stent: follow-up study. *J Vasc Interv Radiol* 1995;6:321–29
13. Palmaz JC, Garcia OJ, Schatz RA, et al. Placement of balloon-expandable intraluminal stents in iliac arteries: first 171 procedures. *Radiology* 1990;174 (3 Pt 2):969–75
14. Kinney TB, Rose SC. Intraarterial pressure measurements during angiographic evaluation of peripheral vascular disease: techniques, interpretation, applications, and limitations. *AJR Am J Roentgenol* 1996;166:277–84
15. Tetteroo E, Haaring C, van der Graaf Y, et al. Intraarterial pressure gradients after randomized angioplasty or stenting of iliac artery lesions: Dutch Iliac Stent Trial Study Group. *Cardiovasc Intervent Radiol* 1996;19:411–17
16. Kadir S, White RI Jr, Kaufman SL, et al. Long-term results of aortoiliac angioplasty. *Surgery* 1983;94:10–14
17. Gu T, Korosec FR, Block WF, et al. PC VIPR: a high-speed 3D phase-contrast method for flow quantification and high-resolution angiography. *AJNR Am J Neuroradiol* 2005;26:743–49
18. Du J, Fain SB, Gu T, et al. Noise reduction in MR angiography with nonlinear anisotropic filtering. *J Magn Reson Imaging* 2004;19:632–39
19. Yang GZ, Kilner PJ, Wood NB, et al. Computation of flow pressure fields from magnetic resonance velocity mapping. *Magn Reson Med* 1996;36:520–26
20. Nasiraei-Moghaddam A, Behrens G, Fatourae N, et al. Factors affecting the accuracy of pressure measurements in vascular stenoses from phase-contrast MRI. *Magn Reson Med* 2004;52:300–09
21. Thompson RB, McVeigh ER. Fast measurement of intracardiac pressure differences with 2D breath-hold phase-contrast MRI. *Magn Reson Med* 2003;49:1056–66
22. Tyszka JM, Laidlaw DH, Asa JW, et al. Three-dimensional, time-resolved (4D) relative pressure mapping using magnetic resonance imaging. *J Magn Reson Imaging* 2000;12:321–29
23. Bland JM, Altman DG. Statistical methods for assessing agreement between two methods of clinical measurement. *Lancet* 1986;1:307–10
24. Bland JM, Altman DG. Measuring agreement in method comparison studies. *Stat Methods Med Res* 1999;8:135–60
25. U-King-Im JM, Trivedi RA, Cross JJ, et al. Measuring carotid stenosis on contrast-enhanced magnetic resonance angiography: diagnostic performance and reproducibility of 3 different methods. *Stroke* 2004;35:2083–88
26. Heiserman JE, Zabramski JM, Drayer BP, et al. Clinical significance of the flow gap in carotid magnetic resonance angiography. *J Neurosurg* 1996;85:384–87